

POD BASED MODEL APPROXIMATION FOR AN INDUSTRIAL GLASS FEEDER

Patricia Astrid[†] Siep Weiland^{*}

^{*} Eindhoven University of Technology, P.O. Box 513, 5600 MB
Eindhoven, The Netherlands

[†] Eindhoven University of Technology, P.O. Box 513, 5600 MB
Eindhoven, The Netherlands

Abstract: This paper describes the application of a model reduction technique based on proper orthogonal decomposition for the modelling of the dynamics of an industrial glass feeder. A technique of missing point estimation is proposed to enhance the computational speed. For a rather complex change of operating conditions, it is shown that the method infers low complexity models of high accuracy. *Copyright*©2005 IFAC

Keywords: Model reduction, proper orthogonal decomposition, industrial applications, glass.

1. INTRODUCTION

Among many glass products, the quality and specifications of container glass mainly depends on the operating conditions of glass melts in industrial glass furnaces. A schematic figure of a glass furnace is given in Figure 1. A typical furnace consists of a melting tank, a working end and a feeder section. The feeder is located between the refiner, where bubbles in molten glass are released and the spout or the glass outlet point, which consists of a dosing mechanism. In the glass melt feeder, the temperature of the glass melt is controlled before the glass exits at the spout where a uniform temperature distribution is desired for the forming process of the glass products. Industrial glass melt feeders are designed to produce glass of different colors, different weights and different viscosity. Among many physical variables, especially the temperature in the melt need to be controlled very tightly both in time as well as in each position of the feeder.

A most critical change of operating conditions of industrial glass feeders involves a color change in the glass melt. Indeed, such a change effects density, viscosity, redox values, conductivity and absorption coefficients, to mention only a few physical parameters.

The control of such a change of operating conditions is a difficult task, especially because the dynamical response of control variables is not, or only partly, understood and because the large transient behavior of such changes have a prolonged effect on the overall performance of the system. A better understanding of the process dynamics for this kind of changes is therefore necessary.

In this paper we consider the reduced order modelling of the temperature changes during color changes in a glass melt feeder. For this we apply the method of proper orthogonal decomposition (POD) which receives increasing interest for industrial applications. The focus on POD techniques for obtaining low complexity models for highly complex dynamic operating conditions of processes is motivated by a number of arguments. Firstly, the POD method is largely application independent. Secondly, the method results in reduced order models that are highly accurate and of very low complexity. Thirdly, unlike many other methods of model approximation the POD technique captures relevant dynamics of the system in a small number of basis functions by explicitly using observed time series or simulated responses of the system. As such, the method is data dependent. Fourthly, the separation of

spatial and temporal dynamics in reduced order models allows a perfect basis for control system design.

In this paper we will apply the POD reduction technique to an industrial glass feeder in describing the dynamics of a setpoint change of a glass feeder from a melt for green container glass to a flint (uncolored) container glass melt. In Section 2 we discuss the model of the feeder. The POD technique is explained in Section 3. Section 4 provides the results of the data acquisition, and reduced order modelling. Conclusions are deferred to Section 6.

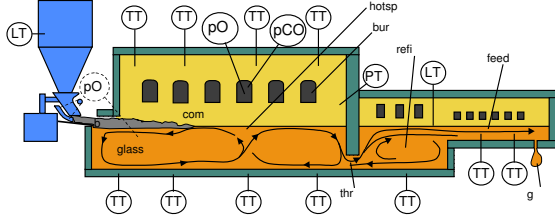


Fig. 1. Glass furnace containing combustion chamber (com), refiner (refi), feeder (feed), and throat (thr)

2. THE MODEL

A schematic view of a glass melt feeder is given in Figure 2. The spatial configuration of the feeder is captured in a subset \mathbb{X} of a three dimensional coordinate system. Here, we consider an industrial feeder for which $\mathbb{X} = [0, 8.5] \times [0, 0.55] \times [0, 2]$ (in meters).

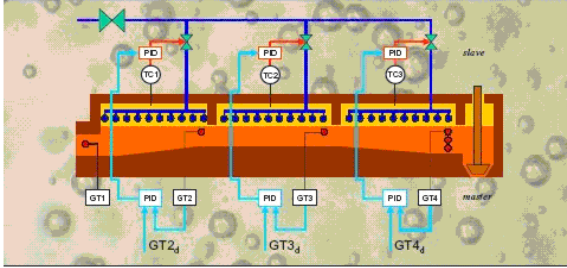


Fig. 2. Schematic view of a glass feeder

In general, the glass melt flow in the feeder can be considered as an incompressible and laminar flow. The governing equations for the feeder are Navier-Stokes equations that describe the velocity field in each direction as well as the pressure field p and the energy equations for the temperature field T (Bird *et al.*, 1960). The Navier-Stokes equations are solved for the glass media only, while the energy equations are solved for heat transfer in the glass melt media, through the feeder walls, and heat transfer from the crown to the melt surface.

The temperature distribution $T(x, t)$ in the feeder is described by the following PDE:

$$\frac{\partial (\rho c_p T)}{\partial t} = -\text{div}(\rho c_p T \mathbf{u}) + \text{div}(\kappa \text{grad} T) + q \quad (1)$$

where ρ is the density, which is temperature dependent for glass, c_p is the heat-capacity, κ is the heat conductivity which is also temperature dependent for glass, and q is the external energy sources applied to the feeder. A complete dynamical model of the feeder is based on Navier Stokes equations for incompressible and laminar flows (Versteeg and Malalasekera, 1995) and includes energy conservation equations, momentum equations, and mass balance equations.

The physical properties (TNO Institute of Applied Physics, 2003) of the green and flint glass are summarized in Table 1 and Table 2. Most physical parameters of the glass melt are functions of temperature. See also (Stanek, 1977), (Beerens *et al.*, 1997) and (Günther and Currie, 1980).

Table 1. Physical parameters green container glass (T is temperature in Kelvin)

Parameters	Green container
Density ρ (kg/m ³)	$2540 - 0.14T$
Viscosity μ (Ns/m ²)	$10^{-2.592} + \frac{4242.904}{T-541.8413}$
Specific heat c_p (J/kg.K)	$1222 + 0.0957T$
Heat conductivity κ (W/mK)	$0.527 + 0.001T + 1.8 \times 10^{-9}T^3$
Absorption coefficient	367.859
Surface emissivity	0.89

Table 2. Physical parameters flint container glass (T is temperature in Kelvin)

Parameters	Flint container
Density ρ (kg/m ³)	$2536 - 0.14T$
Viscosity μ (Ns/m ²)	$10^{-2.490} + \frac{4094.950}{T-553.2733}$
Specific heat c_p (J/kg.K)	$1220 + 0.0957T$
Heat conductivity κ (W/mK)	$0.527 + 0.001T + 2.54 \times 10^{-8}T^3$
Absorption coefficient	26.029
Surface emissivity	0.89

To solve the equations numerically over the spatial domain \mathbb{X} and a finite discrete time domain \mathbb{T} , the feeder is divided into 7128 grid points. Some grid points act as boundary points, where the Dirichlet or Neumann boundary conditions are imposed. These boundary points belong to the input terms. The number of non-boundary points is 3800. Hence, the numerical calculation involves the time evolution of $T(x, t)$ to be computed simultaneously in 3800 positions.

3. MODEL REDUCTION BY PROPER ORTHOGONAL DECOMPOSITION

3.1 Construction of basis functions

The method of proper orthogonal decomposition (POD) amounts to choosing an optimal basis of the space in which the physical variables reside. For the application of this paper, we consider temperatures T defined on a spatial domain \mathbb{X} and a temporal domain \mathbb{T} . It is assumed that for any time $t \in \mathbb{T}$, the spatial temperature distribution $T(\cdot, t)$ mapping \mathbb{X} to \mathbb{R} , belongs to a known separable Hilbert space \mathcal{X} . This means that for some countable index set \mathbb{I} (finite or

infinite) there exists a minimal basis $\{\varphi_i\}_{i \in \mathbb{I}}$ of \mathcal{X} , that is orthonormal in the sense that the inner product $\langle \varphi_i, \varphi_j \rangle$ is 1 if $i = j$ and 0 otherwise. In particular, for any such basis the spatial temperature distribution $T(\cdot, t) \in \mathcal{X}$ (often referred to as the t th *snapshot*) admits a unique expansion of the form

$$T(x, t) = \sum_{i \in \mathbb{I}} a_i(t) \varphi_i(x) \quad (2)$$

where $a_i(t) := \langle \varphi_i, T(\cdot, t) \rangle$ are the (Fourier) coefficients or the *modal coefficients* of the expansion (2). The existence and uniqueness of expansions (2) is therefore the consequence of the assumption that the snapshots belong to a space equipped with the mathematical structure of an inner product. A *time averaging operator* is a linear function $\text{av} : \mathbb{R}^{\mathbb{T}} \rightarrow \mathbb{R}$ with the property that $\min_{t \in \mathbb{T}} f(t) \leq \text{av}(f) \leq \max_{t \in \mathbb{T}} f(t)$. For discrete time sets \mathbb{T} of finite cardinality L one may define, for instance,

$$\text{av}(f) = \frac{1}{L} \sum_{t \in \mathbb{T}} f(t). \quad (3)$$

Now suppose that an ensemble of snapshots $T(x, t)$ with $x \in \mathbb{X}$ and $t \in \mathbb{T}$ is observed, simulated or obtained in an experimental way. The aim will be to accurately approximate T by an expansion that has considerably less terms than (2). An orthonormal basis $\{\varphi_i\}_{i \in \mathbb{I}}$ of \mathcal{X} is said to be a *POD basis* with respect to the observed data T if the Fourier coefficients $a_i(t) = \langle \varphi_i, T(\cdot, t) \rangle$ with $i \in \mathbb{I}$ and $t \in \mathbb{T}$ satisfy

$$\text{av}(a_i^2(t)) \geq \text{av}(a_j^2(t)), \quad \text{whenever } i < j.$$

A POD basis then has the property that for any $n > 0$ the partial sum

$$T_n(x, t) = \sum_{i=1}^n a_i(t) \varphi_i(x) \quad (4)$$

is an optimal approximation of T in the sense that the time-averaged approximation error

$$\text{av}(\|T(x, t) - T_n(x, t)\|^2)$$

with $\|\cdot\|$ the norm induced by the inner product $\langle \cdot, \cdot \rangle$ is minimal among all n th order approximations of the data and among all possible minimal orthonormal bases of \mathcal{X} . It is important to observe that a POD basis is *data dependent*. That is, different data yield different bases. On the other hand, different n do not require different bases for (4) to be optimal (Holmes *et al.*, 1996).

If both \mathbb{X} and \mathbb{T} have finite cardinality, say K and L , then a POD basis is easily constructed from a singular value decomposition of the $K \times L$ data matrix \mathbf{T} whose entries $T_{ij} = T(x_i, t_j)$. Specifically, let $\mathcal{X} = \mathbb{R}^K$ be the Hilbert space with inner product $\langle x_1, x_2 \rangle := x_1^\top x_2$ and suppose that (3) defines the time averaging operator. Let $\mathbf{T} = \Phi \Sigma \Psi^\top$ be a singular value decomposition of \mathbf{T} . Then the j th POD basis function is given by $\varphi_j(x_i) := \Phi_{ij}$, where x_i is an arbitrary element in \mathbb{X} and $j = 1, \dots, K$.

For arbitrary Hilbert spaces \mathcal{X} a POD basis is obtained by constructing the data-correlation map $C :$

$\mathcal{X} \rightarrow \mathcal{X}$ defined by the self-adjoint operator $C(\varphi) := \text{av}(\langle T(\cdot, t), \varphi \rangle T(\cdot, t))$. Then the POD basis are the (normalized) eigenfunctions of C , provided that the operator av commutes with the inner product.

3.2 Construction of modal coefficients

Once the basis functions have been extracted from the data T , then the coefficient functions $a_i(t) := \langle \varphi_i, T(\cdot, t) \rangle$ can be obtained in quite a number of manners. We consider three approaches here.

Galerkin projections. Suppose that the evolution of T is governed by a partial differential equation

$$L(T) = R(T) \quad (5)$$

where $L(T) = \sum_{i=0}^p L_i \frac{\partial^i T}{\partial t^i}$ is a p th order polynomial differential operator and $R(\cdot)$ is a (nonlinear) partial differential operator in the spatial variable. Then the modal coefficients are obtained by requiring that the *Galerkin projection* of the residual $L(T_n) - R(T_n)$ with T_n the partial sum (4) onto the space spanned by φ_i with $i = 1, \dots, n$ vanishes. That is,

$$\langle L(T_n) - R(T_n), \varphi_i \rangle = 0 \quad i = 1, \dots, n. \quad (6)$$

Given the basis functions φ_i , and $n \geq p$, the condition (6) leads to an n -th order *ordinary differential equation* in the coefficients $a_i(t)$ given by

$$L(a_i) = \left\langle R \left(\sum_{j=1}^n a_j(t) \varphi_j(x) \right), \varphi_i(x) \right\rangle$$

where $i = 1, \dots, n$. This defines the dynamics of the model.

Missing point estimation. The coefficients $a_i(t)$ may be inferred from partial information on the spatial domain. Let \mathbb{X}_0 be a strictly proper subset of \mathbb{X} which we will refer to as a *mask*. Let $\mathcal{X}_0 \subset \mathcal{X}$ be the Hilbert space of the restricted mappings $\tilde{T} := T|_{\mathbb{X}_0}$ with $T \in \mathcal{X}$ and let $\tilde{\varphi}_i = \varphi|_{\mathbb{X}_0}$ be the restrictions of the basis functions. Note that $\tilde{\varphi}_i$, $i \geq 1$, will be a basis for \mathcal{X}_0 , but in general this will be neither a minimal nor an orthonormal one. Given an orthonormal basis $\{\varphi_i\}_{i=1}^K$ of \mathcal{X} and a *measurement* \tilde{T} on the mask \mathcal{X}_0 , the objective is to estimate

$$\tilde{T}_n(x, t) = \sum_{i=1}^n \tilde{a}_i(t) \tilde{\varphi}_i(x), \quad x \in \mathbb{X}_0 \quad (7)$$

by minimizing the least squares error

$$E(t) = \|\tilde{T}(x, t) - \tilde{T}_n(x, t)\|_{\mathcal{X}_0}^2 \quad (8)$$

over $\tilde{a}_i(t)$ for $t \in \mathbb{T}$. By deriving $E(t)$ in (8) to $\tilde{a}_i(t)$ and set the derivation to zero, we obtain the optimal estimation of $\tilde{a}_i(t)$ as $\tilde{a}_i^*(t)$:

$$\tilde{a}_i^*(t) \langle \tilde{\varphi}_i(x), \tilde{\varphi}_j(x) \rangle_{\mathcal{X}_0} = \langle \tilde{T}(x, t), \tilde{\varphi}_j(x) \rangle_{\mathcal{X}_0} \quad (9)$$

By solving (9), we obtain the estimate of T by setting

$$\hat{T}_n(x, t) = \sum_{i=1}^n \tilde{a}_i(t) \varphi_i(x), \quad x \in \mathbb{X}.$$

We will refer to \hat{T}_n as the *missing point estimation* of T , based on n modes. The problem of *point selection* amounts to characterizing masks \mathbb{X}_0 of fixed dimension, ℓ say, so that the missing point estimation \hat{T}_n based on the measurement $\tilde{T} = T|_{\mathbb{X}_0 \times \mathbb{T}}$ provides a good estimate of T .

In (Astrid *et al.*, 2004) a criterion is proposed for the selection of such points. The criterion is based on the correlation of the output energy over the spatial domain. Precisely, define for each point $x_k \in \mathbb{X}$, the $L \times L$ matrix $E(x_k)$ whose (i, j) -th entry is

$$E_{ij}(x_k) := \sum_{r=1}^n T(x_r, t_i) T(x_r, t_j) - T(x_k, t_i) T(x_k, t_j). \quad (10)$$

Then, for $k = 1, \dots, K$, define e_k by setting:

$$e_k := \| E(x_k) \| \quad (11)$$

where the norm $\|E\|$ is defined as

$$\|E\| = \sum_{i=1}^L \sum_{j=1}^L E_{ij}^2.$$

Then e_k in (11) represents the total output correlation obtained by ignoring the point $x_k \in \mathbb{X}$. The point with smallest e_k is the one that maximizes the output energy, i.e., the one which is most relevant in comparison with other points. Let us re-index the points in \mathbb{X} as x_{k_1}, \dots, x_{k_K} such that

$$e_{k_1} \leq e_{k_2} \leq \dots \leq e_{k_K}.$$

After this ordering, we will choose the mask $\mathbb{X}_0 = \{x_{k_1}, \dots, x_{k_\ell}\}$. In addition, the re-ordering may take the conditioning of the incomplete basis into account (See (Astrid, 2004)).

The reduced order model by the MPE technique is constructed by projecting the restricted POD basis $\tilde{\Phi}$ onto the equations governing the points in \mathbb{X}_0 . Hence, the term $\tilde{T}(x, t)$ in (9) is replaced by the equation of T located at x .

4. RESULTS

4.1 Collection of data

The color change will significantly change the physical properties of the glass melt. If green container glass melt is replaced by flint (transparent) container glass melt, the heat conductivity will change by a factor 8. The reduced order model will need to take these significant changes into account. If the reduced order model is derived from simulation data where the color change from green to flint is not simulated, then the

reduced order model cannot be expected to accurately capture the color change dynamics.

In this application we focus on the reduced order modeling of the temperature during the color change. The green container glass melt in the feeder is assumed to be initially under the steady state condition with constant pull rate of 80 tons/day and the nominal crown temperature distribution (the inputs) as depicted in Figure 3. The crown temperature of each zone is varied as shown in Figure 3.

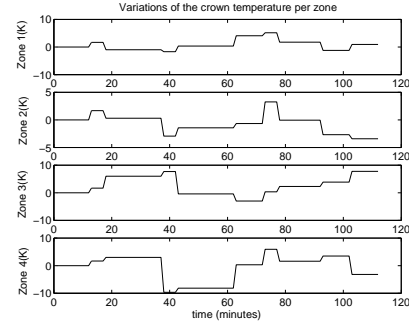


Fig. 3. Crown temperature variations

The green container glass melt is then replaced by the flint container glass melt at time $t = 0$ and data is collected for 112 minutes with a sampling time of 1 minute. To derive the reduced order model of the temperature field, 112 temperature distributions (snapshots) are collected. Hence, $K = 3800$ and $L = 112$. The POD basis functions φ_i defines in Section 2 are computed.

For the color change, 18 POD basis functions are taken. The reduced order model is obtained by employing a Galerkin projection of the first 18 POD basis functions $\varphi_1, \dots, \varphi_{18}$ onto the original model describing the temperature distribution.

4.2 Validation of reduced order model

Figure 4 shows the comparison between the results of the reduced order model and the original model for the measured temperature profiles at the glass melt surface. The points T_1 and T_2 are the measurement points at the surface and the points T_4 to T_5 are the measurement points at the outlet of the furnace. The simulated conditions are the same as when the data was collected. From Figure 4, it is clear that the reduced order model can capture the dynamics of the original model quite well.

The plot of the average absolute error for every grid point is given in Figure 5. The highest value of the absolute error is about 0.08 (in Kelvin), observed in the glass melt. The temperature variations in the glass melt during the simulation is about 20 K. Hence, the deviation of the reduced model from the original model accounts for less than 0.5% of the temperature changes.

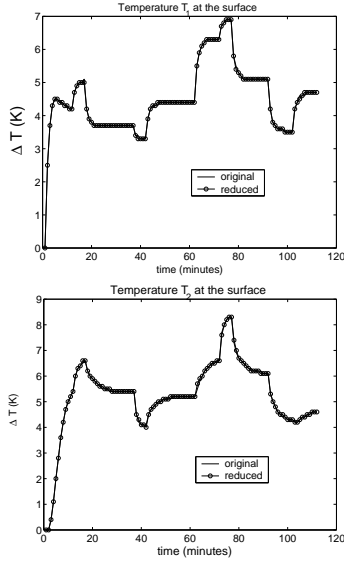


Fig. 4. Reduced and original temperature profiles during color change

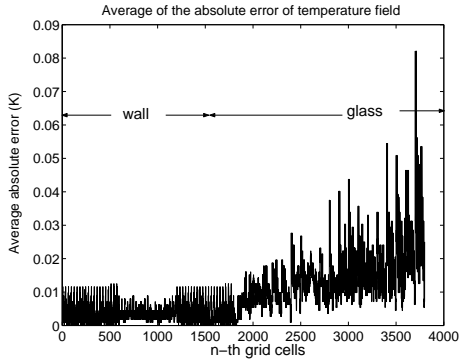


Fig. 5. Absolute errors over the gridpoints

The operating temperature of the glass melt feeder is around 1480 K and the effective heat conductivity of the green container glass is varying around 7 W/m.K. For this operating temperature, the flint container glass melt has an effective heat conductivity of around 84 W/m.K. The drastic change of the glass melt heat conductivity will change the temperature distribution in the glass melt and the resulting transient changes can be captured quite well by the reduced order model.

4.3 Acceleration by missing point estimations

Despite the reduction of complexity, the reduced order model turns out to be about 2.3 times faster in calculation time than the original model. To construct a faster reduced order model, the method of missing point estimation (MPE) as described in section 3.2 is applied.

The selected points \mathbb{X}_0 of the spatial grid consists of the union of two sets. The first being all points adjacent to the points in which on which the crown temperature, inlet temperature and pull rate are defined (the ‘excitation points’ in the feeder, 265 in total).

The second being those points that minimize the MPE criteria as proposed in section 3.2. Since the feeder is symmetric along its width (z -direction), only 1635 points qualify for this.

The value of the criterion e_k is calculated for all 1635 candidate points and shown in Figure 6.

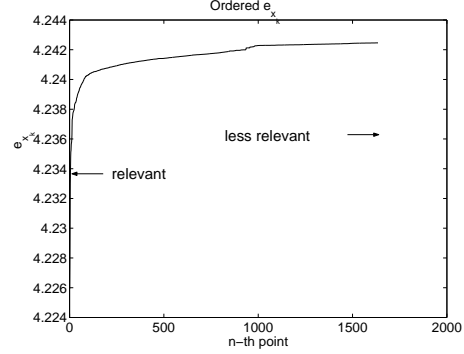


Fig. 6. Ordered values of e_k

Based on these values, the mask \mathbb{X}_0 is then defined by the locations of the 265 excitation points and a number of extra points which are chosen such that the condition number of $\tilde{\Phi}(\mathbb{X}_0)^T \tilde{\Phi}(\mathbb{X}_0)$ is close to 1 with $\Phi(\mathbb{X}_0) = (\varphi_1|_{\mathbb{X}_0} \dots \varphi_n|_{\mathbb{X}_0})$. Based on the condition numbers, 400 additional points have been selected to define a mask \mathbb{X}_0 of 665 points.

The comparisons between the original model, POD model with 18 basis functions, POD-MPE with 665 points and 18 basis functions, and POD-MPE with 465 points and 18 basis functions are depicted in Figure 7 for T_1 and T_2 at the surface.

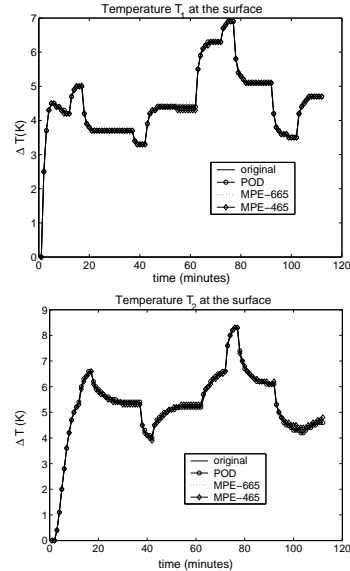


Fig. 7. Reduced and original temperature profiles at the measurement points T_1 and T_2 during the color change simulation.

Table 3 shows the maximum error average (calculated by (5)) and the resulting computational gain with respect to the computing time of the original model

during the situations where the process settings are the same as during the snapshot data collection. From the

Table 3. Comparison between POD and MPE models

Model Type	Maximum average Absolute error	Computational gain
POD	0.081°C	226%
MPE-665	0.082°C	527%
MPE-465	0.13°C	754%

results tabulated in table 3, it is clear the MPE-reduced based model can still follow the dynamics of the original model very well. The resulting reduced order model with MPE based on 465 points is 7.54 times faster than the original model and this corresponds to 8.5 times faster than the real time. Since we only reduce the temperature here and calculate the Navier-Stokes equation by the original model, the enhancement of the computational speed is limited.

To evaluate the performance of the MPE reduced models, we impose random excitation signals at the crown temperature zones. This condition is different to the condition used to derive the POD basis. The random excitation signal is shown in Figure. 8 and applied to all zones.

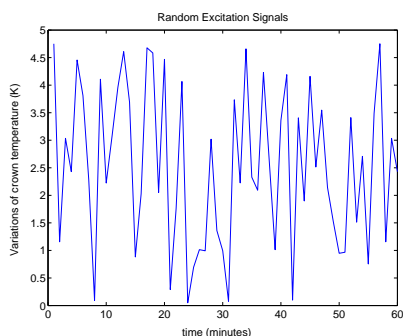


Fig. 8. Random excitation signal for validation of MPE models

The responses of the temperature T_1 and T_2 of both the original and the MPE model with 465 points are shown in Figure. 9. It is obvious from Figure. 9 that the MPE model can still follow the original dynamics quite well despite the fact that the excitation signals are completely different. The absolute error average at these locations account for less than 0.5°C, which is still acceptable for temperature variations of about 8°C.

5. CONCLUSIONS

This paper discusses the reduced order modelling of a glass melt feeder for estimations of the temperature distribution in the glass melt and in the refractory walls. The method of proper orthogonal decomposition is applied to the original feeder model and the results show excellent performance of a reduced order model consisting of only 18 modes.

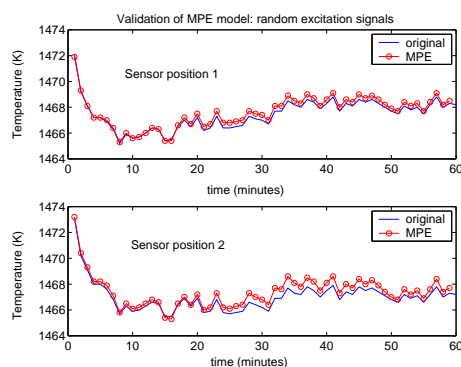


Fig. 9. The validation of the MPE model using random excitation signals

The reduced order model is considerably less complex, but nonlinear, and still computationally expensive. It is for this reason that we also implemented a method of missing point estimation to enhance the computational speed of the reduced order model. Details of the latter method are described in (Astrid *et al.*, 2004).

REFERENCES

- Astrid, P. (2004). Reduction of Process Simulation Models: a Proper Orthogonal Decomposition Approach. PhD dissertation. Eindhoven University of Technology. Department of Electrical Engineering.
- Astrid, P., S. Weiland, K.E. Willcox and A.C.P.M. Backx (2004). Missing point estimation in models described by proper orthogonal decomposition. In: *Proceedings of the 43rd IEEE Conference on Decision and Control*. Bahamas.
- Berkens, R.G.C., H. de Waal and F. Simonis (1997). *Handbook for Glass Technologist*. TNO-TPD Glass Technology. Eindhoven.
- Bird, B.B., W.E. Stewart and E.N. Lightfoot (1960). *Transport Phenomena*. John Wiley and Sons. New York.
- Günther, R. and J. Currie (1980). *Glass-melting tank furnaces*. reprint ed.. Sheffield: Society of glass technology.
- Holmes, P., Lumley and G.Berkooz (1996). *Turbulence, Coherence Structure, Dynamical Systems and Symmetry*. Cambridge University Press. Cambridge.
- TNO Institute of Applied Physics (2003). *X-stream : User Manual, Programmer Manual, Installation Manual, version 2.2*. TNO Institute of Applied Physics. Delft.
- Stanek, J. (1977). *Electric Melting of Glass*. Elsevier. Amsterdam.
- Versteeg, H.K. and W.K. Malalasekera (1995). *An Introduction to Computational Fluid Dynamics, The Finite Volume Method*. Pearson Prentice Hall. Essex.